For hydrocarbon (simplified in this model to just CH_4) concentrations of 1.4 mmol/kg, the maximum W/R is 64, assuming 100% conversion of CO_2 to CH_4 and an initial (but high) CO_2 concentration of ~4000 ppm in the basement rocks (*37*) (fig. S2). This W/R is at the low end of those predicted from the Sr and Nd isotopic compositions of LCHF serpentinites (*37*); however, the samples from seafloor outcrops almost certainly have a reaction history different from that of the rocks directly supplying the present-day fluids at Lost City. More typical and lower initial basement rock CO_2 concentrations would yield lower W/Rs. On the basis of a system constrained by a 400-ppm CO_2 concentration in the basement rocks (*27*) and a conversion of ~50% (as suggested by the He and CO_2 data), we posit that the fluids feeding the LCHF have reacted with rocks in a W/R of less than 5 (fig. S2).

Lost City may be just one of many, as yet undiscovered, off-axis hydrothermal systems. Hydrocarbon production by FTT could be a common means for producing precursors of life-essential building blocks in ocean-floor environments or wherever warm ultramafic rocks are in contact with water.

References and Notes

1. J. L. Charlou, J. P. Donval, Y. Fouquet, B. P. Jean, N. Holm, *Chem. Geol.* **191**, 345 (2002).
2. T. A. Abrajano *et al.*, *Chem. Geol.* **71**, 211 (1988).
3. R. B. Anderson, *The Fischer-Tropsch Synthesis* (Academic Press, Orlando, FL, 1984).
4. D. I. Foustoukos, W. E. Seyfried Jr., *Science* **304**, 1002 (2004).
5. T. M. McCollom, J. S. Seewald, *Earth Planet. Sci. Lett.* **243**, 74 (2006).
6. D. S. Kelley *et al.*, *Nature* **412**, 145 (2001).
7. D. S. Kelley *et al.*, *Science* **307**, 1428 (2005).
8. G. L. Früh-Green *et al.*, *Science* **301**, 495 (2003).
9. J. A. Karson *et al.*, *Geochem. Geophys. Geosyst.* **7**, Q06016 (2006).
10. D. E. Allen, J. Seyfried, W. E. *Geochim. Cosmochim. Acta* **68**, 1347 (2004).
11. R. P. Lowell, P. A. Rona, *Geophys. Res. Lett.* **29**, 1531 (2002).
12. G. Proskurowski, M. D. Lilley, D. S. Kelley, E. J. Olson, *Chem. Geol.* **229**, 331 (2006).
13. M. D. Lilley, D. A. Butterfield, J. E. Lupton, E. J. Olson, *Nature* **422**, 878 (2003).
14. W. E. Seyfried Jr., D. I. Foustoukos, Q. Fu, *Geochim. Cosmochim. Acta* **71**, 3872 (2007).
15. B. Martin, W. S. Fyfe, *Chem. Geol.* **6**, 185 (1970).
16. M. D. Lilley *et al.*, *Nature* **364**, 45 (1993).
17. J. A. Welhan, J. E. Lupton, *AAPG Bull.* **71**, 215 (1987).
18. M. J. Whiticar, *Chem. Geol.* **161**, 291 (1999).
19. B. Sherwood Lollar *et al.*, *Chem. Geol.* **226**, 328 (2006).
20. J. M. Hunt, *Petroleum Geochemistry and Geology* (Freeman, New York, 1996).
21. Y. A. Taran, G. A. Kliger, V. S. Sevastianov, *Geochim. Cosmochim. Acta* **71**, 4474 (2007).
22. B. Sherwood Lollar, T. D. Westgate, J. A. Ward, G. F. Slater, C. G. Lacrampe, *Nature* **416**, 522 (2002).
23. A. Schimmelmann, A. L. Sessions, M. Mastalerz, *Annu. Rev. Earth Planet. Sci.* **34**, 501 (2006).
24. W. F. Giggenbach, *Geochim. Cosmochim. Acta* **61**, 3763 (1997).
25. J. Horita, M. E. Berndt, *Science* **285**, 1055 (1999).
26. P. A. Rona, L. Widenfalk, K. Bostroem, *J. Geophys. Res.* **92**, 1417 (1987).
27. G. L. Früh-Green, J. A. D. Connolly, A. Plas, D. S. Kelley, B. Grobety, in *The Subseafloor Biosphere at Mid-Ocean Ridges*, W. S. D. Wilcock, E. F. Delong, D. S. Kelley, J. A. Baross, C. S. Cary, Eds. (American Geophysical Union, Washington, DC, 2004), vol. 144, pp. 119–136.
28. Low concentrations of CO_2 with large contributions from modern seawater bicarbonate prevent the determination of presumably near–radiocarbon dead end-member ^{14}C contents of Lost City fluids.
29. G. Proskurowski, M. D. Lilley, T. A. Brown, *Earth Planet. Sci. Lett.* **225**, 53 (2004).
30. J. C. Alt, D. A. H. Teagle, *Geochim. Cosmochim. Acta* **63**, 1527 (1999).
31. B. Marty, I. N. Tolstikhin, *Chem. Geol.* **145**, 233 (1998).
32. Seawater bicarbonate accounts for 55 to 98% of the measured CO_2 concentrations in LCHF fluids. The large extrapolations involved in the calculation of end-member CO_2 concentrations introduce large errors that propagate during the determination of end-member $\delta^{13}C\text{-}CO_2$ values by mass-isotope balance. However, measured $\delta^{13}C\text{-}CO_2$ values were −5 to −2‰, indicating mixing between seawater bicarbonate (−0.40‰) and an end-member more depleted in ^{13}C. The best-quality sample yielded an end-member $\delta^{13}C\text{-}CO_2$ value of −8.7 ± 1.5‰, and samples with greater uncertainties had lower values.
33. D. S. Kelley, G. L. Früh-Green, *Geochim. Cosmochim. Acta* **65**, 3325 (2001).
34. W. J. Brazelton, M. O. Schrenk, D. S. Kelley, J. A. Baross, *Appl. Environ. Microbiol.* **72**, 6257 (2006).
35. M. O. Schrenk, D. S. Kelley, S. A. Bolton, J. A. Baross, *Environ. Microbiol.* **6**, 1086 (2004).
36. D. S. Kelley, G. L. Früh-Green, *J. Geophys. Res.* **104**, 10439 (1999).
37. A. Delacour, P. Schaeffer, S. M. Bernasconi, G. L. Früh-Green, *Eos Trans. AGU* **87**, B31B (2006).

38. We thank the captains and crews of the R/V *Atlantis* and R/V *Ronald H. Brown*, and the crews of the DSV *Alvin* and the ROV *Hercules* for their indispensable expertise in deep-sea oceanography. We also thank R. Ballard and the Institute for Exploration for their efforts during the 2005 Lost City expedition, a proof-of-concept cruise directed by satellite-linked shore-based investigators. This work was supported in part by NSF grant OCE0137206, the NOAA Ocean Exploration Program, and a fellowship from the Woods Hole Oceanographic Institution Deep Ocean Exploration Institute. We thank D. Butterfield for providing Mg data. This manuscript benefited greatly from the comments by two anonymous reviewers.

Supporting Online Material

www.sciencemag.org/cgi/content/full/319/5863/604/DC1
Materials and Methods
Figs. S1 and S2
Tables S1 and S2
References

1 October 2007; accepted 14 December 2007
10.1126/science.1151194

Prioritizing Climate Change Adaptation Needs for Food Security in 2030

David B. Lobell,[1,2]* Marshall B. Burke,[1] Claudia Tebaldi,[3] Michael D. Mastrandrea,[4] Walter P. Falcon,[1] Rosamond L. Naylor[1]

Investments aimed at improving agricultural adaptation to climate change inevitably favor some crops and regions over others. An analysis of climate risks for crops in 12 food-insecure regions was conducted to identify adaptation priorities, based on statistical crop models and climate projections for 2030 from 20 general circulation models. Results indicate South Asia and Southern Africa as two regions that, without sufficient adaptation measures, will likely suffer negative impacts on several crops that are important to large food-insecure human populations. We also find that uncertainties vary widely by crop, and therefore priorities will depend on the risk attitudes of investment institutions.

Adaptation is a key factor that will shape the future severity of climate change impacts on food production (*1*). Although relatively inexpensive changes, such as shifting planting dates or switching to an existing crop variety, may moderate negative impacts, the biggest benefits will likely result from more costly measures including the development of new crop varieties and expansion of irrigation (*2*). These adaptations will require substantial investments by farmers, governments, scientists, and development organizations, all of whom face many other demands on their resources. Prioritization of investment needs, such as through the identification of "climate risk hot spots" (*3*), is therefore a critical issue but has received limited attention to date.

We consider three components to be essential to any prioritization approach: (i) selection of a time scale over which impacts are most relevant to investment decisions, (ii) a clear definition of criteria used for prioritization, and (iii) an ability to evaluate these criteria across a suite of crops and regions. Here, we focus on food security impacts by 2030: a time period most relevant to large agricultural investments, which typically take 15 to 30 years to realize full returns (*4*, *5*).

We consider several different criteria for this time scale. First is the importance of the

[1]Food Security and Environment Program, Woods Institute for the Environment and the Freeman Spogli Institute for International Studies, Stanford University, Stanford, CA 94305, USA. [2]Lawrence Livermore National Laboratory (LLNL), Livermore, CA 94550, USA. [3]National Center for Atmospheric Research, Boulder, CO 80305, USA. [4]Woods Institute for the Environment, Stanford University, Stanford, CA 94305, USA.

*To whom correspondence should be addressed. E-mail: dlobell@stanford.edu

crop to a region's food-insecure human population [hunger importance (HI)]. Second is the median projected impact of climate change on a crop's production by 2030 (indicated by C50), assuming no adaptation. For this analysis, we generate multiple (i.e., 100) projections of impacts based on different models of climate change and crop response, in order to capture relevant uncertainties. The projections are then ranked, and the average of the 50th and 51st values are used as the median. A third criterion is the fifth percentile of projected impacts by 2030 (where C05 indicates the fifth value of the ranked projections), which we use to represent the lower tail or "worst case" among the projections. Finally, we consider the 95th percentile of projected impacts by 2030 (where C95 indicates the 95th value of the ranked projections), which we use to represent the upper tail or "best case" among the projections.

We first identified 12 major food-insecure regions, each of which (i) comprise groups of countries with broadly similar diets and agricultural production systems and (ii) contain a notable share of the world's malnourished individuals as estimated by the Food and Agriculture Organization (FAO) (Table 1; see fig. S1 for details on regions). For each region, we computed the HI value for each crop by multiplying the number of malnourished individuals by the crop's percent contribution to average per capita calorie consumption [see supporting online material (SOM) Text S1 and table S1]. A hunger importance ranking (HIR) was then generated by ranking the HI values for all crop-by-region combinations. Rice, maize, and wheat contribute roughly half of the calories currently consumed by the world's poor and only 31% of the calories consumed by those in sub-Saharan Africa, illustrating the importance of considering additional crops in food security assessments. The use of projected malnourished populations in 2030 rather than current population values had a very small influence on the rankings (table S2).

Several options exist for evaluating climate change impacts across a suite of crops and regions (SOM Text S2). We used data sets on historical crop harvests (*6*), monthly temperatures and precipitation, and maps of crop locations to develop statistical crop models for 94 crop-region combinations spanning the 12 study regions (see SOM Text S3; results summarized in Table 1). Of these combinations, 46% (43) exhibited a statistically significant model ($P < 0.05$), and 22% (21) had a model R^2 of at least 0.3. As seen in the examples for wheat in South and West Asia (fig. S3), in some cases the model's strength came primarily from a (typically negative) temperature effect on yield, whereas, in other cases, a (typically positive) rainfall effect provided most of the explanatory power.

The crop temperature sensitivities estimated by the statistical models were compared with corresponding values from previous studies that relied on established process-based models within the same regions (SOM Text S4). Our statistical estimates generally overlapped the lower end of the range of previous estimates, indicating that impacts estimated by the statistical models may be considered conservative but in reasonable agreement with estimates from process-based approaches.

To project climate changes for the crop regions, along with their uncertainties, we used output from 20 general circulation models (GCMs) that have contributed to the World Climate Research Programme's Coupled Model Intercomparison Project phase 3 (WCRP CMIP3) (*7*). Median projections of average temperature change from 1980–2000 to 2020–2040 were roughly 1.0°C in most regions, with few models projecting less than 0.5°C warming in any season and some models warming by as much as 2.0°C (Fig. 1A). In contrast to the unanimous warming, models were mixed in the direction of simulated precipitation change. All regions had at least one model with positive and one model with negative projected precipitation changes, with median projections ranging from about –10% to +5% (Fig. 1B). Some relevant tendencies of current GCMs, as noted in (*8*), are toward precipitation decreases during December to February (DJF) in South Asia and Central America, precipitation decreases in June to August (JJA) in Southern Africa, Central America, and Brazil, and precipitation increases in DJF in East Africa.

We estimated a probability distribution of production changes for 2030 (the average from

Table 1. Regions evaluated in this study and selected summary statistics. Countries within each region are indicated in the SOM.

Region	Code	Malnourished		Crops modeled	Crops with significant model*
		Millions of people	World total (%)		
South Asia	SAS	262.6	30.1%	9	7
China	CHI	158.5	18.2%	7	2
Southeast Asia	SEA	109.7	12.6%	7	4
East Africa	EAF	79.0	9.1%	10	2
Central Africa	CAF	47.6	5.5%	8	0
Southern Africa	SAF	33.3	3.8%	8	6
West Africa	WAF	27.5	3.2%	8	2
Central America and Caribbean	CAC	25.4	2.9%	5	2
Sahel	SAH	24.9	2.9%	7	7
West Asia	WAS	21.9	2.5%	10	4
Andean region	AND	21.4	2.5%	9	3
Brazil	BRA	13.5	1.6%	6	4
Total	ALL	825.3	94.7%	94	43

*A model was judged significant if it explained more than 14% of variance in yield or production ($R^2 > 0.14$). This threshold was based on the 95th percentile of the R^2 statistic from a Monte Carlo experiment, which computed 1000 multiple regression models for a randomly generated 42-year time series with two random predictor variables.

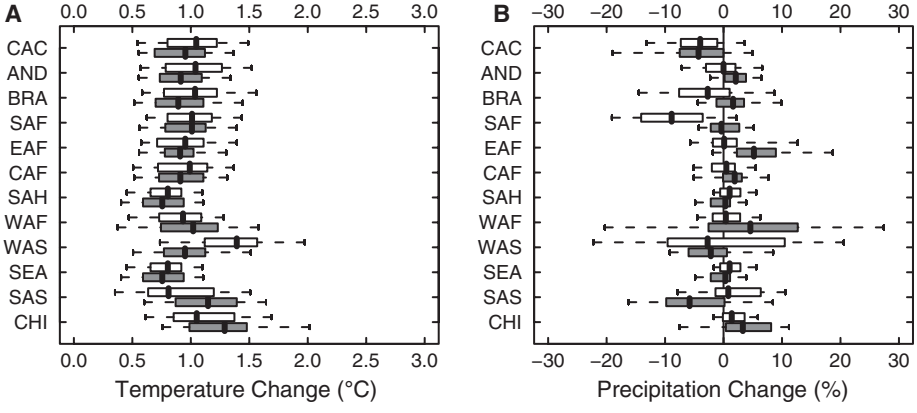

Fig. 1. Summary of projected (**A**) temperature (°C) and (**B**) precipitation (%) changes for 2030 (the averages from 2020 to 2039 relative to those from 1980 to 1999) based on output from 20 GCMs and three emission scenarios. Gray boxes show DJF averages and white boxes show JJA averages. Dashed lines extend from 5th to 95th percentile of projections, boxes extend from 25th to 75th percentile, and the middle vertical line within each box indicates the median projection.

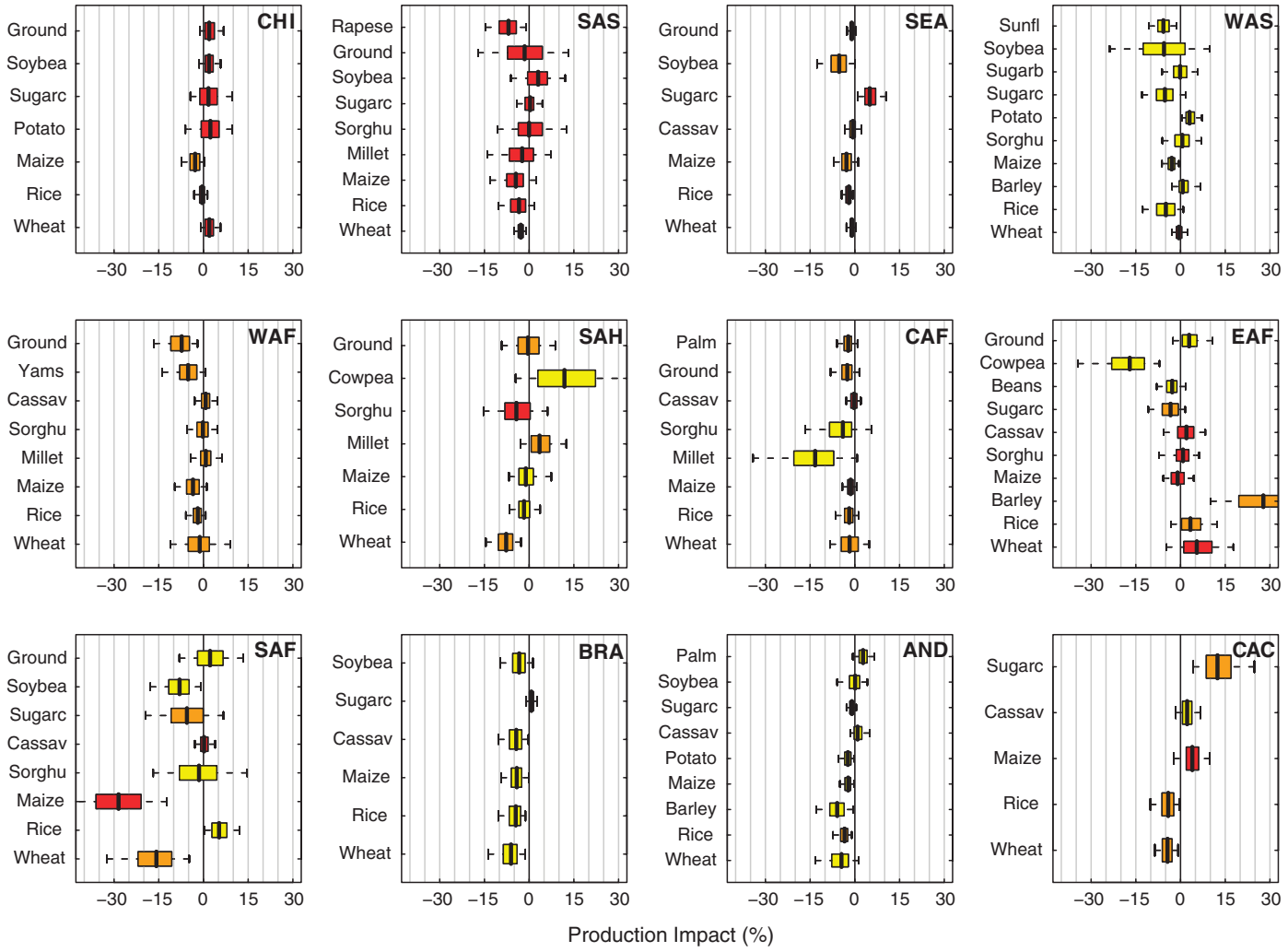

Fig. 2. Probabilistic projections of production impacts in 2030 from climate change (expressed as a percentage of 1998 to 2002 average yields). Red, orange, and yellow indicate a HIR of 1 to 30 (more important), 31 to 60 (important), and 61 to 94 (less important), respectively. Dashed lines extend from 5th to 95th percentile of projections, boxes extend from 25th to 75th percentile, and the middle vertical line within each box indicates the median projection. Region codes are defined in Table 1.

Table 2. Crop priority lists based on different criteria. C05 = 5th percentile of projected impacts (5th lowest out of 100 projections); C50 = 50th percentile (median); C95 = 95th percentile. Results are shown only for the HIR = 1 to 30 and HIR = 31 to 60 categories.

HIR value	Criterion	Crops
1 to 30	C05 < −10%	South Asia millet, groundnut, rapeseed; Sahel sorghum; Southern Africa maize
	C50 < −5%	South Asia rapeseed; Southern Africa maize
	C95 < 0%	South Asia wheat; Southeast Asia rice; Southern Africa maize
31 to 60	C05 < −10%	Southeast Asia soybean; West Asia rice; Western Africa wheat, yams, groundnut; Sahel wheat; East Africa sugarcane; Southern Africa wheat, sugarcane; Brazil wheat, rice; Andean Region wheat; Central America rice
	C50 < −5%	Southeast Asia soybean; West Asia rice; Western Africa yams, groundnut; Sahel wheat; Southern Africa wheat, sugarcane; Brazil wheat
	C95 < 0%	Western Africa groundnut; Sahel wheat; Southern Africa wheat; Brazil wheat, rice; Central America wheat, rice

2020 to 2039 relative to that from 1980 to 1999) for each crop using a Monte Carlo procedure that propagated both climate and crop uncertainties (*9*). To facilitate comparison between crops and regions, we expressed production changes for all crops as a percentage of average values for 1998 to 2002. The impact projections are summarized in Fig. 2.

For simplicity, we consider three general classes of projections. First, several projections (e.g., Southern Africa maize and wheat) are consistently negative, with an estimated 95% or greater chance that climate changes will harm crop production in the absence of adaptation (C95 < 0). These cases generally arise from a strong dependence of historical production variations on temperature, combined with projected warming large enough to overwhelm the uncertain impacts of precipitation changes.

Second, there are many cases with large uncertainties, with model impacts ranging from substantially negative to positive (e.g., South Asia groundnut, Southern Africa sorghum). These cases usually arise from a relatively strong dependence of historical production on rainfall, combined with large uncertainties in future precipitation changes. More precise projections of precipitation would therefore be particularly useful to reduce impact uncertainties in these situations. Large uncertainties also arise in some cases (e.g., cowpea in East Africa) from an estimated production response to historical temperature that is strongly negative but also highly uncertain.

Finally, there are many cases characterized by a narrow 90% confidence interval of impacts within ±5% of zero. In a few cases, such as wheat in West Asia, this reflects a strong effect of historical rainfall variations (fig. S1), combined with a relatively narrow range of rainfall projections during the growing season (Fig. 1; West Asia wheat is grown in DJF). In most cases, such as cassava in West Africa, the narrow confidence intervals result from a relatively weak relationship between historical production and growing-season climate. Therefore, we can only say that the likely impacts appear small, given the current data sets and models used to describe crop responses to climate. In cases with low model R^2, approaches other than the FAO-based regression models used here may be more appropriate.

Based on the above projections, we identified a small subset of crops that met different prioritization criteria (Table 2). First, crops were separated into groups of "more important" (HIR = 1 to 30), "important" (HIR = 31 to 60), and "less important" (HIR = 61 to 94). Within each category, we identified crops below three thresholds: the first corresponding to instances where at least 5% of the models predicted greater than 10% loss of production (C05 < –10%), the second to where at least half the models projected greater than a 5% production loss (C50 < –5%), and the third to where at least 95% of the models predicted some production loss (C95 < 0%).

Although several crops met more than one of these criteria, such as maize in Southern Africa and rapeseed in South Asia, the varying estimates of uncertainty for different crops, in general, resulted in noticeable differences when prioritizing crops on the basis of the three different thresholds (Table 2). For example, a relatively weak relationship was found between values at the two tails of the projection distributions—C05 and C95—across all crops (fig. S4). This result indicates a need to explicitly consider uncertainty and risk attitudes when setting priorities, which is an issue that has received limited attention (*10*).

Because attitudes toward risk differ, and given that impact projections for some crops are more uncertain than those for other crops, various institutions might derive different priorities from the results in Table 2. For example, one set of institutions might wish to focus on those cases where negative impacts are most likely to occur, in order to maximize the likelihood that investments will generate some benefits. By this criterion (C95 < 0%), South Asia wheat, Southeast Asia rice, and Southern Africa maize appear as the most important crops in need of adaptation investments.

Others might argue that adaptation activities that do not account for worst-case projections will be inadequate in the face of low-probability, high-consequence climate impacts: that is to say, investments should target those crops and regions for which some models predict very negative outcomes. A different subset of crops is identified for this criterion (C05 < –10%), with several South Asian crops, Sahel sorghum, and (again) Southern Africa maize appearing as the most in need of attention.

Either of these risk attitudes could be applied with an explicit regional focus. For a sub-Saharan African institution interested in investing where negative impacts are most likely to occur [where median impact projections are substantially negative (C50 < –5%) or where most climate models agree that negative impacts are likely to occur (C95 < 0%)], priority investments would include Southern Africa maize, wheat, and sugarcane, Western Africa yams and groundnut, and Sahel wheat.

Despite the many assumptions and uncertainties associated with the crop and climate models used (SOM Text S5), the above analysis points to many cases where food security is clearly threatened by climate change in the relatively near-term. The importance of adaptation in South Asia and Southern Africa appears particularly robust, because crops in these regions appear for all criteria considered here (Table 2). The results also highlight several regions (e.g., Central Africa) where climate-yield relationships are poorly captured by current data sets, and therefore future work in this regard is needed to inform adaptation efforts.

Impacts will likely vary substantially within individual regions according to differences in biophysical resources, management, and other factors. The broad-scale analysis presented here was intended only to identify major areas of concern, and further studies at finer spatial scales are needed to resolve local hot spots within regions. Consideration of other social and technological aspects of vulnerability, such as the existing adaptive capacity in a region or the difficulty of making adaptations for specific cropping systems, should also be integrated into prioritization efforts. Although we do not attempt to identify the particular adaptation strategies that should be pursued, we note that, in some regions, switching from highly impacted to less impacted crops may be one viable adaptation option. In this case, the identification of less impacted crops is another valuable outcome of a comprehensive approach that simultaneously considers all crops relevant to the food-insecure.

References and Notes

1. W. Easterling *et al.*, in *Climate Change 2007: Impacts, Adaptation and Vulnerability. Contribution of Working Group II to the Fourth Assessment Report of the Intergovernmental Panel on Climate Change* (Cambridge Univ. Press, Cambridge, 2007), pp. 273–313.
2. C. Rosenzweig, M. L. Parry, *Nature* **367**, 133 (1994).
3. I. Burton, M. van Aalst, "Look before you leap: A risk management approach for incorporating climate change adaptation in World Bank operations" (World Bank, Washington, DC, 2004).
4. J. M. Alston, C. Chan-Kang, M. C. Marra, P. G. Pardey, T. J. Wyatt, "A meta-analysis of rates of return to agricultural R&D: Ex pede Herculem?" (International Food Policy Research Institute, Washington, DC, 2000).
5. J. Reilly, D. Schimmelpfennig, *Clim. Change* **45**, 253 (2000).
6. We used FAO data on national crop production and area, which include quantities consumed or used by the producers in addition to those sold on the market.
7. Model simulations under three SRES (Special Report on Emissions Scenarios) emission scenarios corresponding to relatively low (B1), medium (A1b), and high (A2) emission trajectories were used. Although the mean projections for the emission scenarios exhibit very small differences out to 2030, the use of three scenarios provided a larger sample of simulations with which to assess climate uncertainty. For all simulations, average monthly output for 1980–1999 was subtracted from that of 2020–2039 to compute monthly changes in temperature and precipitation.
8. J. H. Christensen *et al.*, in *Climate Change 2007: The Physical Science Basis. Contribution of Working Group I to the Fourth Assessment Report of the Intergovernmental Panel on Climate Change*, S. Solomon *et al.*, Eds. (Cambridge Univ. Press, Cambridge, 2007), pp. 847–940.
9. Namely, the crop regression model was fit with a bootstrap sample from the historical data, and the coefficients from the regression model were then multiplied by projected changes in average temperature and precipitation, which were randomly selected from the CMIP3 database. This process was repeated 100 times for each crop. Bootstrap resampling is a common approach to estimate uncertainty in regression coefficients, although this addresses only the component of model uncertainty that arises from a finite historical sample and not the potential uncertainty from structural errors in the model. Similarly, the representation of climate uncertainty by equally weighting all available GCMs is a common approach but could potentially be improved, such as by weighting models according to their agreement with the model consensus and with historical observations. Nonetheless, the resulting probability distributions incorporate reasonable measures of both climate and crop uncertainty, and thus should fairly reflect both the absolute and relative level of uncertainties between crops.
10. B. Smit *et al.*, in *Climate Change 2001: Impacts, Adaptation and Vulnerability. Contribution of Working Group II to the Third Assessment Report of the Intergovernmental Panel on Climate Change* (Cambridge Univ. Press, Cambridge, 2001), pp. 877–912.

11. We thank D. Battisti, C. Field, and three anonymous reviewers for helpful comments. D.B.L. was supported by a Lawrence Fellowship from LLNL. Part of this work was performed under the auspices of the U.S. Department of Energy (DOE) by LLNL under contract DE-AC52-07NA27344. We acknowledge the modeling groups, the Program for Climate Model Diagnosis and Intercomparison, and the WCRP's Working Group on Coupled Modelling for their roles in making available the WCRP CMIP3 multimodel data set. Support of this data set is provided by the Office of Science, DOE.

Supporting Online Material

www.sciencemag.org/cgi/content/full/319/5863/607/DC1
SOM Text S1 to S5
Figs. S1 to S5
Tables S1 to S3
References

30 October 2007; accepted 18 December 2007
10.1126/science.1152339

Prioritizing Climate Change Adaptation Needs for Food Security in 2030

David B. Lobell, Marshall B. Burke, Claudia Tebaldi, Michael D. Mastrandrea, Walter P. Falcon and Rosamond L. Naylor

Science **319** (5863), 607-610.
DOI: 10.1126/science.1152339